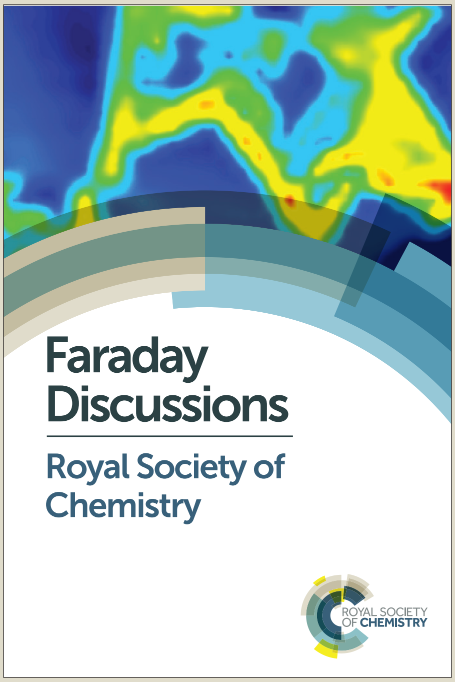
Faraday
Discussions
Royal Society of
Chemistry
ROYAL SOCIETY OF CHEMISTRY

Analyzing fractal gel of charged oblate nanoparticles in suspension using time resolved rheometry and DLVO theory

*Shweta Jatav and Yogesh M. Joshi**

Department of Chemical Engineering

Indian Institute of Technology, Kanpur, Kanpur -208016

Corresponding author email id: joshi@iitk.ac.in

Abstract:

The disk-like nanoparticles of Laponite are known to self-assemble to form a fractal gel within hours after sufficiently large concentration of the same is dispersed in water containing salt. A concentration of sodium counter-ions associated with Laponite particles, however, continue to increase over a period of days suggesting delamination of Laponite disks from stacks is sluggish or/and dissociation of counter-ions is slow. In either case, spontaneous self-assembly of Laponite particles occur even though delamination and/or counter-ion dissociation has not reached its equilibrium state. In order to obtain nature of fractal gel as the extent of delamination and/or dissociation progresses towards equilibrium, we subject the Laponite suspension to freezing – defrosting cycle, which interestingly reinitiates the gelation process in suspension afresh. Application of time resolved rheometry to defrosted suspension shows that iso-frequency loss tangent curves intersect at an identical point validating the Winter – Chambon criterion for a critical fractal gel state. Interesting while time required to form critical gel is observed to decrease with increase time elapsed since preparation at which freezing- defrosting is carried out, the fractal dimension of the critical gel is observed to remain unaffected. We also solve DLVO theory for free energy interactions between the negatively charged Laponite particles faces and analyze the observed phenomena.

1 Introduction

Colloidal particles suspended in aqueous media arrange themselves in variety of microstructures depending upon their concentration, nature of charges present on the particles, and nature and concentration of electrolytes.[1] Colloidal suspensions are used in variety of applications including that in medicines, soaps and detergents, inks and paints, lotions and pastes, as a variety of food items, etc. Microstructure of colloidal suspension on one hand determines its application; while on the other hand, it also determines its long term stability against sedimentation, creaming or thixotropic cake formation. In the limit of low concentrations the colloidal suspension usually remains in a liquid state for a long time.[2] However, with increase in concentration their tendency to self-assemble increases. Sometimes the self-assembled structures are out of thermodynamic equilibrium and evolve with time in search of more stable states.[3] Presence of anisotropic shape and dissimilar charges add further to the intricate inter-particle interactions. In this work we study self-assembly of nanoparticles of Laponite, a synthetic clay mineral, which has disk like shape with dissimilar charges distribution when dispersed in aqueous media. Laponite in aqueous media has been used in variety of industries including pharmaceutical, paper, paint, home care, personal care, petrochemical, agrochemical, etc., primarily as a rheology modifier.[4-6] In academics, due to its spectacular time dependent physical properties, aqueous Laponite suspension has been termed as a model soft glassy material.[7] In the literature, this system has been proposed to show a rich array of microstructures. In this work we employ rheological tools to gain further insight into its microstructure after subjecting it to freezing – defrosting cycle.

Laponite clay, with chemical formula of unit cell $Na_{+0.7}[(Si_8Mg_{5.5}Li_{0.3})O_{20}(OH)_4]_{-0.7}$, has a disk-like shape with thickness of 1 nm and 25±2 nm diameter.[8] Laponite belongs to a family of 2:1 polysilicate wherein one octahedral layer of magnesium oxide is sandwiched between two tetrahedral layers of silica. In the middle layer some magnesium atoms are replaced by lithium, which gives a negative charge on the faces of Laponite particle. This charge is compensated by sharing sodium atoms in the interlayer spacing between the particles of Laponite. In a dry state Laponite particles are present in the form of stacks. When Laponite powder is dispersed in water, it enters the interlayer gallery causing the stacks to swell.[9, 10] During this process stacks of Laponite particles with variety of sizes are present in water.[9] On one hand these stacks undergo swelling, while on the other hand Laponite particles on the surface of the stacks delaminate as a function of time.

Suspension of Laponite in water is known to show spectacular increase in elastic modulus as a function of time, eventually acquiring a soft solid like consistency.[11-14] It is typically observed that ionic conductivity of suspension increases very slowly over a timescale of days after preparation of the same.[11, 15, 16] The increase in ionic conductivity is due to dissociation of Na^+ ions from the faces of Laponite. Since significant dissociation of Na^+ ions occurs only after delamination of individual Laponite particles from the stacks, sluggishness of either or of both the processes could lead to slow enhancement of ionic conductivity. Possibility of both the processes being slow has been speculated in the literature.[11, 17] The edges of the Laponite particles where crystal structure is broken primarily contain Mg-OH groups, whose charge depends upon the pH. Point of zero charge for Mg-OH is around 12.5,[18] below which the edges acquire positive charge due to protonation of the same. Overall, negatively charged faces, positively charged edges and anisotropic shape of Laponite particle lead to complex interparticle interactions, which include edge to face attraction as well as face to face repulsion.[11, 19, 20] Presence of externally added salt in a suspension increases concentration of ions, which are known to shield the charges on the particles.[11, 21]

Owing to presence of dissimilar charges, the microstructure of Laponite suspension influenced by repulsive as well as attractive interactions present in between the Laponite particles. Many versions of Laponite suspension phase diagram as a function of salt (NaCl) and Laponite concentration have been proposed in the literature.[19, 22-24] Laponite suspension shows phase separation below around 1 weight % or in a limit of very high salt concentrations (>20 mM).[19, 24] Furthermore, while there is a consensus that between 1 and 2 weight % aqueous suspension of Laponite forms a colloidal gel, microstructure above concentration of 2 weight % is a matter of debate. Ruzicka and coworkers[25] by carrying out small angle X-Ray scattering (SAXS) proposed that for suspensions with concentration greater than 2 weight % Laponite particles forms a glass state in which particle jammed in space, remaining untouched with other particles.[25] Interestingly Ruzicka and coworkers[26] indicated that while repulsion dominates the early stages after preparation of Laponite suspension, attraction among the particles play a significant role as a suspension ages.

Ruzicka and coworkers also carried out Monte Carlo simulations, wherein disk-like particles with charged patches (three positive potentials on edge and one negative potential on each of the two faces) interact with each other.[27, 28]

Interestingly the structure factor obtained from simulations showed similarity with that obtained from SAXS measurements. In an alternate proposal Mongondry and coworkers[24] proposed Laponite suspension to exist in a gel state wherein particles form a space spanning network by forming edge to face attractive bonds. Interestingly Joshi and coworkers[11, 29, 30] through series of papers on rheological, dynamic light scattering and electrochemical experiments showed that rate of structural build-up in Laponite suspension increases with decrease in repulsive screening length related with the Laponite particle faces. Consequently, they claimed the resultant structure cannot be merely repulsion dominated but the attractive interactions must have profound influence on the same over all the timescales since preparation of the same. It should be noted that gel formation in aqueous media is not just limited to Laponite. The other types of clays such as bentonite, montmorillonite, nontronite, etc., which are structurally similar to Laponite, have also been reported to form attractive gels when suspended in water.[10, 31, 32] Clays modified by hydrophobic chains render it compatibility with organic solvents. Such clay dispersions have also been observed to undergo sol-gel transition.[33, 34] However this topic is beyond the scope of present work.

A gel state and a glass state is distinguished from each other by a length-scale above which density of the same becomes homogeneous.[3] In glasses, this length-scale is of the order of an average inter-particle distance, while in case of gels this length-scale is much greater than an average inter-particle distance. This length-scale can usually be obtained by scattering as well as microscopic techniques.[19, 35] Rheologically, on the other hand, there are unique signatures to recognize a point of glass transition compared to that of the critical gel state. A point of glass transition, wherein liquid undergoes ergodicity breaking, depends on timescale of observation. Consequently, rheological properties at glass transition depend on frequency.[36] Typically at a point of glass transition $\tan\delta$, which is the ratio of G'' (viscous modulus) to G' (elastic modulus), shows a maximum. For molecular glasses, a glass transition temperature (associated with maximum in $\tan\delta$) is observed to increase with increase in frequency applied to monitor the evolution.[37] The critical gel state, on the contrary, is that state when particles just form a space spanning percolated network. The point at which such network is formed is independent of time scale of observation or applied frequency.[38] Winter and Chambon[39] in a seminal paper proposed that at the critical gel point, elastic $\left(G'\right)$ and viscous $\left(G''\right)$ modulus show identical frequency $\left(\omega\right)$ dependence given by:

$$G' = G'' \cot\left(n\pi/2\right) = \frac{\pi S}{2\Gamma(n)\sin\left(n\pi/2\right)}\omega^{n}, \qquad (1)$$

where $\Gamma(n)$ is an Euler gamma function of power law exponent n and S is the gel strength. Consequently at the critical gel state $\tan\delta = \tan\left(n\pi/2\right)$ is independent of frequency. Therefore, rheologically the critical gel state is identified as the point at which iso-frequency $\tan\delta$ curves meet.[38] Beyond the critical gel state, a gel consolidates wherein inter-particle bonds become stronger along with alteration of the network.[40]

The critical gel state that validates Winter – Chambon criterion has been observed for a large number of crosslinking polymeric materials[41-44] and colloidal particulate materials undergoing gelation.[45-47] Interestingly the knowledge of n also leads to obtain fractal dimension of the critical gel.[48] Remarkably fractal dimensions obtained from independent small angle X-Ray scattering measurements on polymeric[49] as well as colloidal[50] gels closely match that obtained from the rheology experiments. Interestingly dependence of G' on ω given by equation (1) yields relaxation time spectrum, given by $H\left(\tau\right) \sim \tau^{-n}$, where τ is relaxation time. Very recently Winter[51] proposed that the behavior of relaxation time spectrum at a point of glass transition shows positive slope when $H\left(\tau\right)$ is plotted as a function of τ on a double logarithmic scale. This is contrary to the behavior that observed at the critical gel state, thereby indicating an important criterion to distinguish both the states.

In order to check validity of Winter – Chambon criterion given by equation (1), a system evolving as a function of time is usually subjected to time resolved rheometry, wherein frequency sweep is applied in a continuous succession. Cocard and coworkers[52] were the first to investigate aqueous suspension of Laponite using time resolved rheometry to validate the Winter – Chambon criterion. More recently Jatav and Joshi[53] validated presence of critical gel state for a freshly prepared 2.8 weight % Laponite suspension with 3 mM NaCl, which is expected to be consisting network formed by bonds between positive edges and negative faces.[10] Interestingly, while the critical gel state is observed within few hours of mixing Laponite in water, slow dissociation of Na^+ ions continues over timescale of days.[11, 15] Consequently, the critical gel state observed for a freshly prepared Laponite suspension is associated with only partial dissociation of Na^+ ions and/ or partial delamination of particles.

As mentioned before, the negative potential on the faces of Laponite particles is a consequence of dissociation of Na^+ ions.[11, 30] Furthermore, concentration of Na^+ ions in the electric double layer surrounding a particle also influences width of the same which strongly influences inter-particle attractive as well as repulsive interactions.[1, 11] Discussion in previous paragraphs therefore suggests that at the time of critical gel formation either delamination of Laponite particles and/or the dissociation of Na^+ ions from the faces of Laponite particles did not reach the equilibrium. As a result, the observed critical gel state is associated with that of only a partly evolved delamination/dissociation dynamics. It is possible that the nature of gel state could have been different if sufficient time would have been given first for the delamination/dissociation process to reach equilibrium followed by gelation of the particles. However, a process of colloidal gelation such as in case of Laponite suspension, unlike chemical gelation,[54] cannot be stopped or paused at any point by killing the bond formation process.

It has been observed that application of strong deformation field induces gel – to – liquid transition in a colloidal gel.[3] Subsequent to cessation of deformation, the rheological properties of Laponite suspension evolve as a function of time, whose dynamics is qualitatively similar to that of evolution in freshly prepared suspension.[7, 13] It may, therefore, appear that nature of critical gel state could be studied by shear melting a Laponite suspension after dissociation/delamination process has reached the equilibrium. However it has been observed that shear melting does not obliterate all the inter-particle bonds formed during a process of gelation.[11, 53] Consequently post shear melting restructuring of Laponite suspension does not sample the critical gel state.[53] The deviation from the critical gel state becomes so severe with age, at which the shear melting is applied, such that for a sufficiently old shear melted Laponite suspension, iso-frequency $\tan\delta$ curves do not even cross each other.[46, 53]

The objective of the present work is to explore possibility of obtaining nature of the critical gel state at various concentrations of dissociated Na^+ ions until its equilibrium value if reached, which also guarantees delamination to be nearly complete. In order to achieve the same, we freeze a Laponite suspension below 0°C and after holding it there for some time, defrost it. Since, at 0°C relative permittivity of ice is smaller than that of liquid water by over a factor of 25, defrosted samples are in completely collapsed state. The gelation of such samples leads to characterization of the critical gel point at various intermediate states of partial dissociation and/or delamination.

2 Sample Preparation and Experimental Protocol

Laponite XLG used in this study was obtained from BYK Additives, Ltd. A protocol to prepare 2.8 weight % Laponite suspension with 3 mM NaCl in water having pH 10 is same as that reported by Jatav and Joshi,[53] which involved vigorous mixing of mentioned ingredients with oven dried Laponite using turrex drive for 30 min. The freshly prepared suspension was stored in air-tight polypropylene bottles in constant temperature chamber maintained at 30˚C. The sample was stored for various rest times (t_R), and rheological, conductivity and pH measurements were carried out on the same. The suspension was observed to remain chemically and physically stable over a duration of all the experiments, wherein no dissolution of magnesium ions and no phase separation were observed.[55]

Rheological experiments were carried out in concentric cylinder geometry (outer diameter of 30 mm and gap of 1 mm) of DHR3 rheometer (TA instruments). Suspension was loaded into shear cell using a dropper, and an oscillatory stress of 25 Pa at 0.1 Hz frequency was applied for 5 min during which sample underwent shear melting leading to a steady value of complex viscosity and strain magnitude. Subsequently the suspension was frozen to –10˚C and after maintaining it at that temperature for 90 min it was defrosted to 30˚C. After reaching thermal equilibrium at 30˚C, sample was again subjected to 25 Pa oscillatory stress at 0.1 Hz frequency for 5 min to assess the effect of freezing. Next an oscillatory stress of 0.1

Pa with frequency varying in a range: 0.5-25 rad/s was applied to the sample in a continuous succession. The ionic conductivity was measured using DS-71 conductivity meter with 2 pole cell electrode, while pH was measured using F-71 pH meter with standard glass electrode (Both the instruments from HORIBA Scientific). Before measuring ionic conductivity and pH, the suspension was mechanically rejuvenated to convert it into a liquid, which facilitates unhindered ionic mobility.

3 Results and discussion

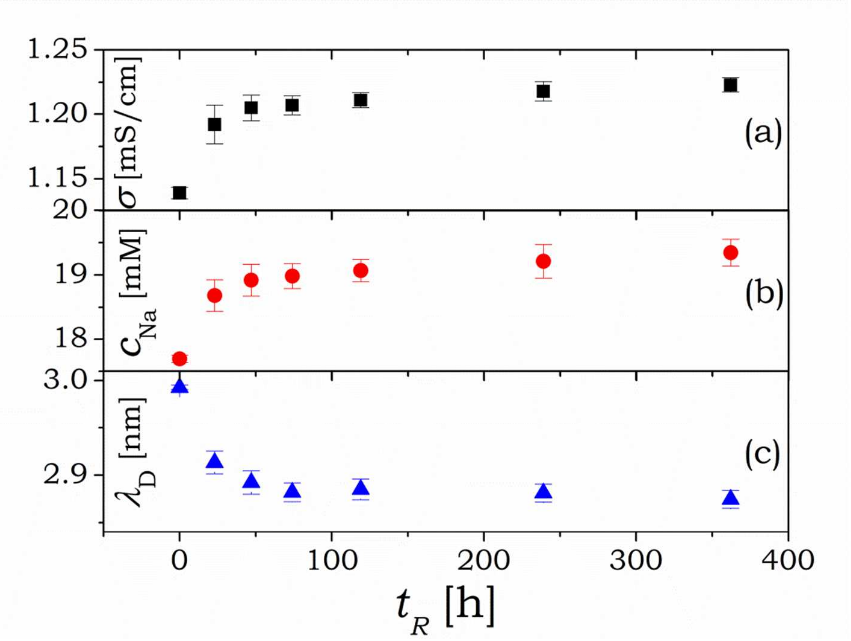

Figure 1. (a) The ionic conductivity (σ), (b) concentration of Na$^+$ ion (c_{Na}) and (c) the Debye screening length (λ_D) is plotted as a function of rest time (t_R) of the suspension. It can be seen that after 100 h all the three variables attain the equilibrium value.

The ionic conductivity (σ) of the suspension measured before freezing on various days elapsed since preparation (t_R) is plotted in figure 1(a). It was observed that freezing – defrosting has practically no effect on σ, which is measured at 30°C after defrosting the suspension. It can be seen that, just after preparation, value of σ is small but increases rapidly with increase in t_R. However beyond t_R=50 h increase in σ becomes weak as a function of t_R and shows a sign of reaching a constant value. As mentioned before, increase in σ over a prolonged period could arise from delayed delamination of Laponite plates, and/or sluggish dissociation of Na$^+$ counter ions. The ionic conductivity is directly related to mobility and concentration of various ionic species in a suspension and is given by:[56]

$$\sigma = e\sum_i \mu_i c_i \,, \tag{2}$$

where e is electron charge (1.602×10^{-19} C), while μ_i and c_i are respectively the mobility and concentration of ith ionic specie. In aqueous Laponite suspension studied in the present work various ionic species present are: Na$^+$, Cl$^-$ and OH$^-$ ions. The concentration of OH$^-$ ions (c_{OH}) can be calculated from the pH of suspension while concentration of Cl$^-$ ions (c_{Cl}) is same as concentration of externally added NaCl (3 mM). In principle H$^+$ ions are also present, however since pH of suspension is always around 10.3 over the explored duration, contribution of H$^+$ ion is negligibly small. With knowledge of μ_i of the mentioned ionic species, concentration of Na$^+$ ions (c_{Na}) can be easily calculated from equation (2). In figure 1(b), c_{Na} is plotted as function of t_R. It can be seen that, as expected, c_{Na} follows the same trend as that of σ.

The knowledge of c_i also enables us to estimate the Debye screening length (λ_D) associated with the electric double layer on the faces of Laponite particles, and is given by:

$$\lambda_D = \left\{ \frac{\varepsilon_0 \varepsilon_r k_B T}{e^2 \sum_i z_i^2 c_i} \right\}^{1/2} , \tag{3}$$

where ε_0 is permittivity of free space, ε_r is relative permittivity of water, k_B is Boltzmann constant, T is temperature, and z_i is ionic charge number of ith specie. In figure 1(c) λ_D is plotted as a function of t_R. It can be seen that λ_D decreases strongly over first 50 h followed by a weak decrease to reach a constant value. The decrease in λ_D can be attributed to increase in concentration of Na$^+$ ions in the bulk of suspension which compresses the electrostatic double layer around the particle faces.

The energy interactions between two clay particles approaching each other in a parallel fashion as a function of normal distance between the two faces ($2d$) is obtained by solving DLVO (due to Derjaguin, Landau, Verwey and Overbeek) theory.[1] In the DLVO theory, the total free energy (V_T) is obtained by adding contributions from electrostatic (usually repulsive, V_E) and van der Waals (attractive, V_{vdW}) interactions between the faces separated by distance $2d$ and is given by:

$$V_T = V_E + V_{vdW} = \left(64 c_{\mathrm{Na}} k_B T \lambda_D\right) \tanh^2\left(z/4\right) \exp\left(\frac{-2d}{\lambda_D}\right) - \frac{A_H}{48\pi d^2}, \qquad (4)$$

In equation (4) the terms on the right side are respectively the expressions of free energy for electrostatic and van der Waals interactions. Parameter z is a dimensionless number related to surface charge density (ς) given by:

$$\sinh\left(z/2\right) = \left(8 c_{\mathrm{Na}} \varepsilon_o \varepsilon_r k_B T\right)^{-1/2} \varsigma, \qquad (5)$$

while A_H is the Hamaker constant whose value is 1.06 $\times 10^{-20}$ J for Laponite.[57] In equation (5) ς is obtained by knowing number of Na^+ ions dissociated per face of Laponite particle, and is given by

$$\varsigma = e\left(c_{Na} - c'_{Na}\right) / \left(2 A_L n_p\right), \qquad (6)$$

where c'_{Na} is Na^+ ions concentration due to external sources such as NaCl and NaOH added to the suspension. Furthermore, surface area of one face of Laponite particle is given by A_L while n_p is number density of Laponite particles, so that denominator of equation (6) is the total surface area of all the faces of Laponite particles considering the same to be completely delaminated. However, as mentioned above this may not be the case, particularly in the initial period after preparation. In such case equation (6) will provide a lower bound on ς so that the actual value will always be greater than or equal to the estimated value of ς, and difference between them will decrease with t_R. Moreover, in the literature it has been proposed that the negative charge on the faces of clay particles exposed by dissociation of counter-ions attracts H^+ ions from the bulk.[58] However since suspension pH is around 10.3, concentration of H^+ ions in the bulk is extremely small. We, therefore, expect alteration of surface charge density due to adsorption of H^+ ions from bulk to be negligible.

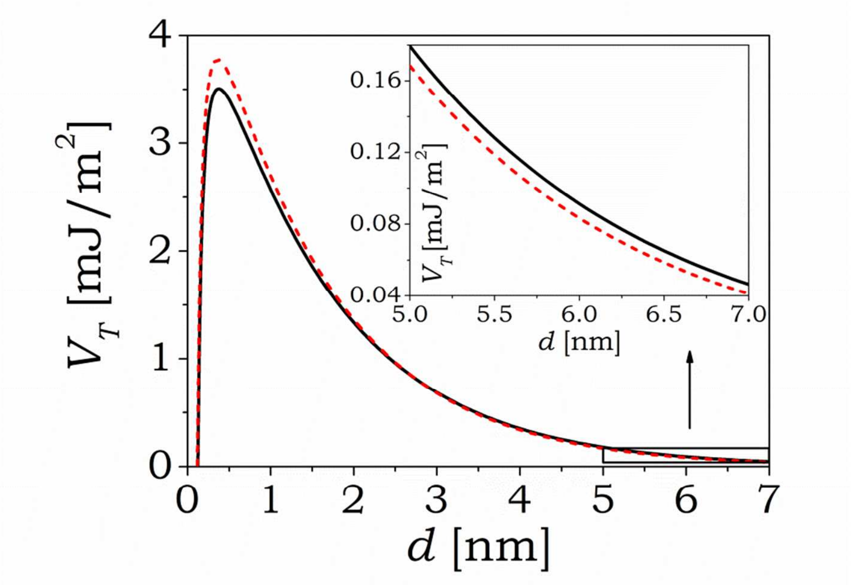

Figure 2. The free energy of interactions obtained from DLVO theory, when two Laponite particles move toward each other face – to – face, is plotted as a function of half of normal distance between the same for two rest times: full line t_R=0 h and dashed line t_R=362 h. The inset shows the enlarged view of a tail.

In figure 2, we plot the total interaction energy V_T obtained from equation (4) as a function of d for the two values of t_R. It can be seen that owing to like charges on the faces of Laponite, when particles approach each other face – to – face by remaining parallel, repulsion increases with decrease in d, and reaches a maximum at small values of d before decreasing due to van der Waals interactions. From equations (4) and (5) it is apparent that the height of repulsive energy barrier is proportional to ς and $c_{\mathrm{Na}}^{0.5}$ (as λ_D is proportional to $c_{\mathrm{Na}}^{-0.5}$), consequently height of repulsive energy barrier increases with t_R as shown in figure 2. As mentioned above estimated value of ς associated with the faces of the particles is a lower estimate. In a limiting assumption that the dissociation of Na^+ ions is instantaneous, the upper bound of ς will be always a constant. However, even in such limit c_{Na} would increase with t_R. Consequently for all the scenarios, with controlling step being delamination, dissociation or combination of both, maximum height of repulsive energy barrier will always increase with t_R. The width of the decaying repulsive barrier with increase in inter-plate distance, on the other hand, is governed by $\exp\left(-2d/\lambda_D\right)$, and therefore faster decay is observed with increase in t_R as shown in the inset of figure 2.

The repulsive interaction shown in figure 2 is associated with face – to – face parallel arrangement of plates. However in a suspension the particles may approach each other in any orientation. With increased electronegativity of the faces, decreased width of repulsive barrier, and possibly increased number density of Laponite particles due to delamination, rate of positive edge to negative face bond formation is expected to increase at higher values of t_R. Consequently gelation is expected to be faster at higher values of t_R. Moreover, all the above mentioned effects are also expected to influence structure of the fractal gel.

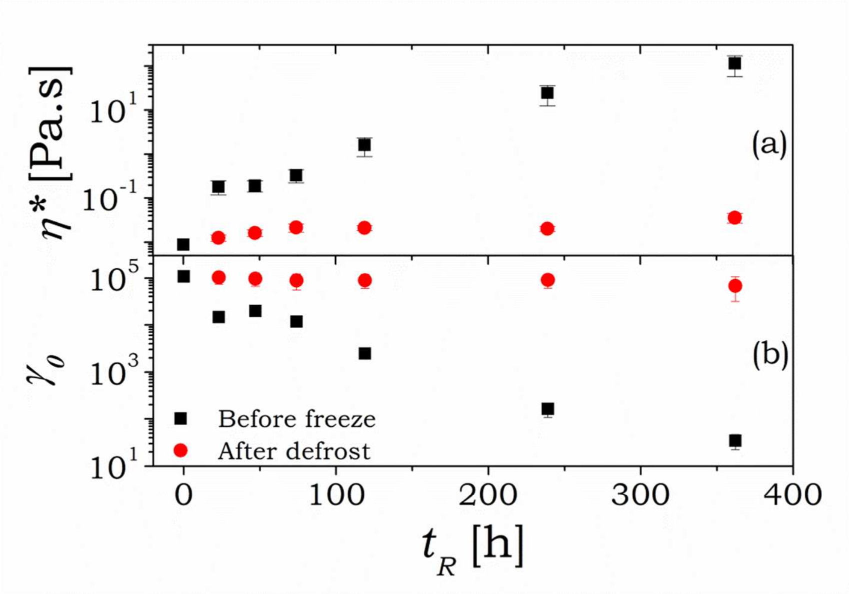

Figure 3. The steady state values of (a) complex viscosity (η^*) and (b) magnitude of strain (γ_0) under magnitude of oscillatory stress of 25 Pa at 0.1 Hz frequency are plotted as a function of rest time (t_R) before freezing (squares) and after defrosting (circles).

We study the nature of critical gel using time resolved rheometry. A sample, which was aged over rest time t_R, was loaded into the shear cell, and after attaining thermal equilibrium at 30°C, subjected to shear melting as mentioned before. Owing to aging over the duration of t_R, material acquires high viscosity and elastic modulus. However during shear melting complex viscosity (η^*) of suspension decreases while magnitude of oscillatory strain (γ_0) increases, and both the variables eventually reach a plateau. In figure 3, plateau value of η^* and γ_0 are plotted as a function of t_R. It can be seen that plateau value of η^* increases while that of γ_0 decreases with increase in t_R. This is because the shear melting cannot completely break the structure formed during aging that occurs over a rest time (t_R). The extent of unbroken structure increases with t_R causing respectively increase and decrease in plateau values of η^* and γ_0.

Subsequent to shear melting, temperature of a sample was decreased to –10°C and held there for 90 min, after which temperature was again raised to 30°C. The temperature of –10°C was chosen because presence of Laponite and salt decrease the freezing point of suspension to –8°C. The values of η^* and γ_0 of defrosted samples is also plotted in figure 3, which clearly show respectively very small and large values for η^* and γ_0 that are almost independent of t_R. Tremendous drop in viscosity of a defrosted state compared to that of completely shear melted state of a same sample suggests complete collapse of the structure during freezing – defrosting cycle, which could not achieved by shear melting. We believe that this due to significant change in relative permeability of ice and water. Upon increasing temperature of frozen Laponite suspension, in the vicinity of melting point ice surrounding Laponite particles undergo phase transformation from solid to liquid. Since the relative permittivity of liquid water at freezing point is 88 while that of ice is 3.2, presence of crystallites along with water obstruct the electrostatic interactions, which is the very backbone of the structure. Consequently, after defrosting, suspension acquires a liquid state of low viscosity with Laponite particles undergoing Brownian motion as shown in figure 3. The viscosity of defrosted suspension being independent of t_R clearly suggests obliteration of structure is indeed through. This behavior is in contrast with that observed during shear melting, wherein progressively lesser obliteration occurs with increase in t_R.

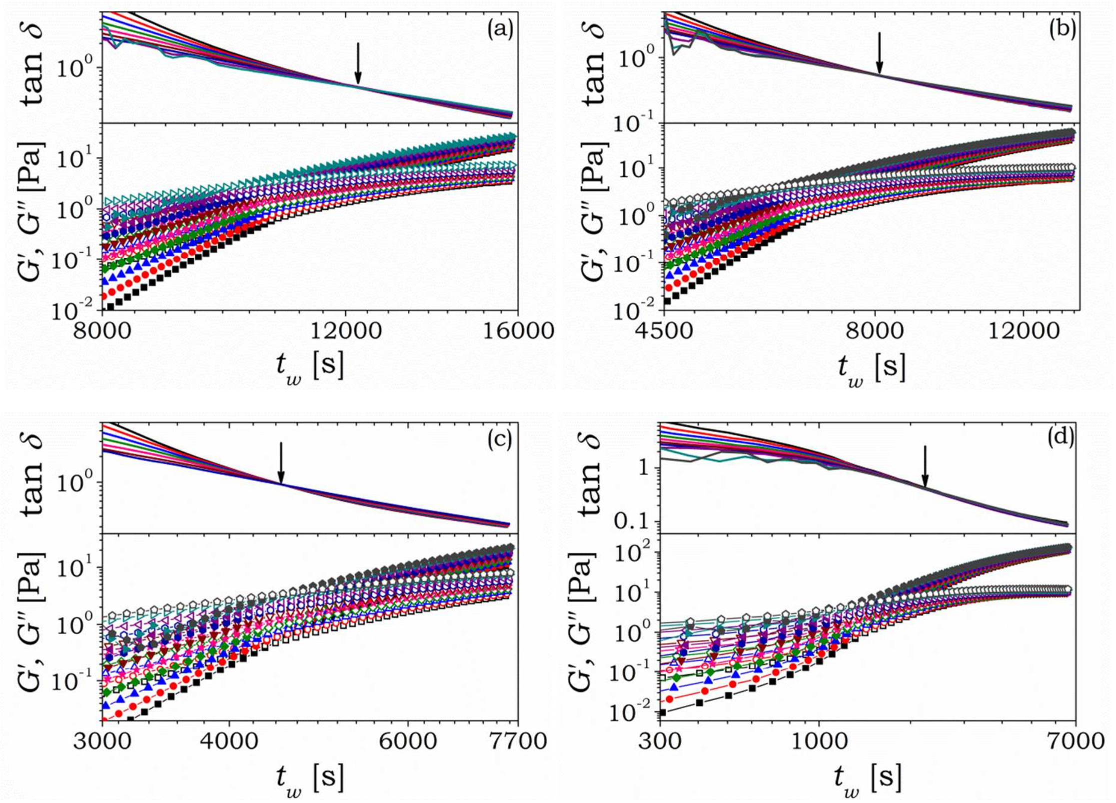

Figure 4. The elastic modulus (G', filled symbols), viscous modulus (G'', open symbols) and loss tangent ($\tan\delta$) are plotted as a function of time elapsed since defrosting (t_w) for different rest time (t_R)= (a) 0 h, (b) 47 h, (c) 119 h and (d) 362 h. In all the G' and G'' plots frequency increase from bottom to top (0.5, 0.8, 1.25, 2, 3.15, 5, 8, 12.5, 20, and 25 rad/s) and for $\tan\delta$ increase in frequency from top to bottom is applicable before the critical gel point. The critical gel point has been shown by a vertical arrow.

Subsequent to defrosting, we subject the sample to cyclic frequency sweep in the linear viscoelastic domain. The corresponding evolution of G', G'' and $\tan\delta$ is plotted in figure 4 as a function of time elapsed since defrosting (t_w) for four different t_R. After defrosting $G' << G''$ irrespective of frequency, suggesting a sample to be in a liquid state. Both the moduli increase as a function of time with G' increasing at a faster rate than G'' so that they eventually cross each other. However with decrease in frequency the crossover point $(G' = G'')$ gets delayed in time. Rapid increase in G' compared to G'' leads $\tan\delta$ to decrease with time, but with lesser intensity with increase in frequency. Consequently all the iso-frequency $\tan\delta$ curves intersect with each other, but importantly at the identical point. Such unique intersection point irrespective of frequency is a characteristic feature of critical gel state as proposed by the Winter – Chambon criterion.[54] We also subjected samples older than 20 days to freezing – defrosting cycle. However, upon defrosting the suspensions with t_R >20 day, while undergo liquid to solid transition, it do not show a critical gel state. In this case all the decreasing iso-frequency $\tan d$ curves simply approach each other as a function of time without crossing each other. We believe that such behavior could arise from sintering of some of the clay particles with each other over a long time, which cannot be broken to individual particle level upon freezing-defrosting leading to the observed behavior.

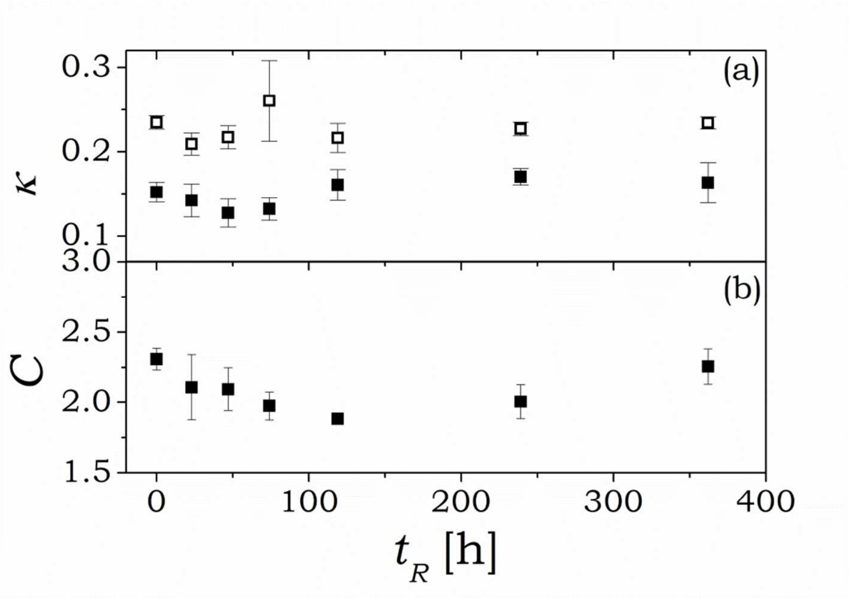

Figure 5. The parameters (a) dynamic critical exponent (κ) (filled symbols obtained from G' and open symbols obtained from G'') and (b) proportionality constant (C) as defined by equation (7) are plotted as a function of rest time (t_R). Both the parameters show remarkably close match to that of critical gels of polymeric materials.

For polymeric gels, the rate of change in G' and G'' near the gel point is observed to show a power law dependence on frequency (ω) given by:[59]

$$\left(\frac{\partial \ln G'}{\partial t}\right)_{t=t_g} \cong C\left(\frac{\partial \ln G''}{\partial t}\right)_{t=t_g} \quad : \quad \omega^{-\kappa}, \qquad (7)$$

where C is proportionality constant and κ is dynamic critical exponent. Interestingly, for a variety of polymer gels (polymer gels containing different polymer – solvent pairs as well as within same a polymer-solvent pair variation of chain length, concentration and stoichiometry) κ is observed to be within a range: 0.22 ± 0.02.[46, 59-62] Even for physical gels value of κ is observed to be in the similar range.[46] In addition the proportionality constant C has been reported to be around 2 for various chemical as well as physical gel systems.[46, 59] In figure 5, we plot κ and C as a function of t_R. Remarkably C is indeed observed to be around 2, while κ calculated from a rate of change of G'' is observed to be in between 0.2 to 0.25 while κ calculated from rate of change of G' is around 0.15. Figure 5, therefore indicates a very close match between values of κ and C observed for various chemical and physical gels and the defrosted aqueous suspension of Laponite studied in this work.

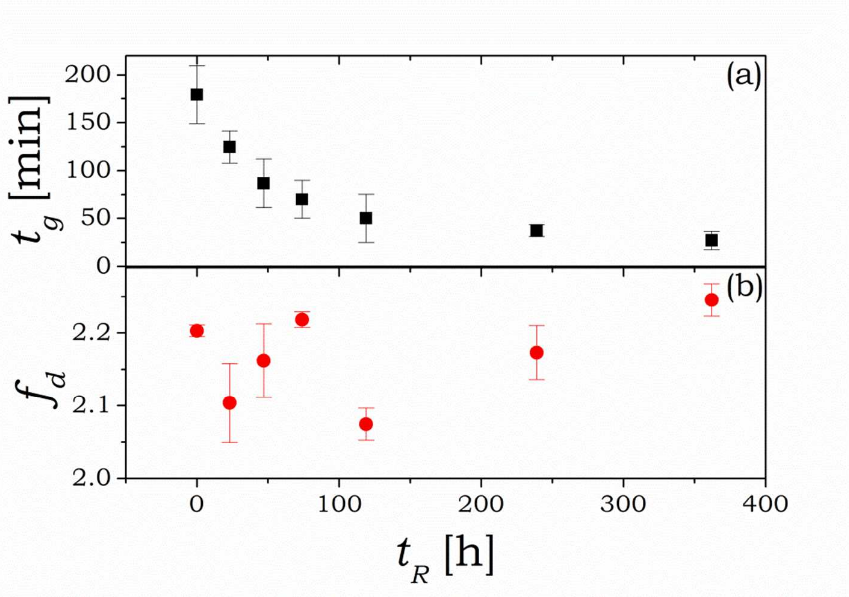

Figure 6. (a) The time to gelation (t_g) and (b) fractal dimension (f_d) are plotted as a function of rest time (t_R). While t_g decreases, f_d remains constant within an uncertainty window.

Figure 4 clearly shows that the critical gel point occurs at earlier times with increase in t_R. In figure 6 we plot time to gelation (t_g) as a function of t_R, which shows a sharp decreases with increase in t_R for t_R<100 h. However at higher t_R, decrease in t_g becomes weaker. From equation (1) a value of $\tan\delta$ associated with the critical gel point leads to critical relaxation exponent n. The critical gel is known to have a fractal structure and in a seminal contribution Muthukumar[48] obtained a relationship between exponent n and fractal dimension f_d by accounting for excluded volume interaction; and for a d dimensional system it is given by:[48]

$$f_d = \frac{(d+2)(2n-d)}{2(n-d)}. \qquad (8)$$

We obtain f_d from equation (8) for $d=3$, which is also plotted in figure 6 as a function of t_R. Interestingly it can be seen that, unlike time to gelation (t_g), fractal dimension f_d remains practically constant in the vicinity of 2.2 over the explored range of t_R.

The results of rheological study in the light of DLVO theory lead to an interesting scenario. The results of DLVO theory, clearly show that the height of repulsive energy barrier (and/or negative charge on the faces) increases while its width (: λ_D) decreases with t_R. This trend clearly suggests that at higher t_R Laponite particles are more prone to form bonds when they approach each other in a non-parallel fashion leading to faster gel formation as resulted in decrease in t_g. However faster dynamics of critical gel formation with possibly more delaminated particles and/or increase in concentration of dissociated counter-ions does not seem to be affecting a fractal dimension of the critical gel. It is generally observed that faster gel formation, because of fewer attempts for inter-particle bond formation as typically is the case in diffusion-limited cluster aggregation (DLCA), leads to more open structure (low fractal dimension in the range 1.7 to 1.9).[63] On the other hand more attempts to form inter particle bonds when repulsive barrier is significant enough leads to reaction-limited cluster aggregation (RLCA) which leads to compact structure with higher fractal dimension (typically above 2). However in the present case, decrease in t_g by a factor 6 does not influence the fractal dimension with all the values remaining in the window of 2.1 to 2.3. This suggests that particles still need more attempts to form the inter-particle bonds, which can be attributed to repulsive barrier among the particles, leading to compact structure formation through RLCA.

4. Conclusions

In this work we investigate aqueous suspension of 2.8 weight % Laponite with 3 mM NaCl, which spontaneously self-assembles to form a fractal gel within few hours of preparation. On the other hand, the delamination of stacks of Laponite and/or dissociation of counter-ions from the faces of the same, progress over the timescale of days. Since delamination of particles and dissociated Na^+ counter-ions is expected to have a profound effect on the nature of fractal gel, we subject Laponite suspension to freezing – defrosting cycle, which reinitiates the gelation process in the same afresh but at a maturated state of delamination/dissociation. Application of cyclic frequency sweep to the defrosted suspension shows formation of critical fractal gel. Interestingly, while the time required to form the critical gel decreases with increase rest time at which it is subjected to freezing – defrosting cycle, the fractal dimension of the critical gel remains unaffected. With the knowledge of concentration of various ionic species in suspension we obtain Debye screening length on the faces of the particles. We also solve DLVO theory between the faces of Laponite particles when they approach each other in a parallel fashion. DLVO theory suggests that the particles must overcome a repulsive energy barrier whose height grows but width shrinks with rest time. Consequently formation of fractal gel, whose building block is considered to be edge to face bond gets, accelerated leading to faster gel formation as observed in the rheology experiments. However, even though the increase in rest time causes greater delamination of stacks of Laponite particles and/or dissociation Na^+ ions, the fractal dimension of the critical gel is observed to remain unaffected.

Acknowledgements

We acknowledge the financial support from the Department of Atomic Energy–Science Research Council (DAE-SRC), Government of India.

References

1. J. N. Israelachvili, *Intermolecular and Surface Forces*, Academic Press, London, 3 edn., 2010.
2. R. G. Larson, *The Structure and Rheology of Complex Fluids*, Clarendon Press, Oxford, 1999.
3. Y. M. Joshi, *Annual Review of Chemical and Biomolecular Engineering*, 2014, **5**, 181.
4. M. Ghadiri, H. Hau, W. Chrzanowski, H. Agus and R. Rohanizadeh, *RSC Advances*, 2013, **3**, 20193-20201.
5. K. Sun and S. R. Raghavan, *Langmuir*, 2010, **26**, 8015-8020.
6. Negrete, J.-M. Letoffe, J.-L. Putaux, L. David and E. Bourgeat-Lami, *Langmuir*, 2004, **20**, 1564-1571.
7. A. Shahin and Y. M. Joshi, *Langmuir*, 2012, **28**, 5826-5833.
8. M. Kroon, W. L. Vos and G. H. Wegdam, *Phys. Rev. E*, 1998, **57**, 1962-1970.
9. Y. M. Joshi, *J. Chem. Phys.*, 2007, **127**, 081102.
10. H. Van Olphen, *An Introduction to Clay Colloid Chemistry*, Wiley, New York, 1977.
11. A. Shahin and Y. M. Joshi, *Langmuir*, 2012, **28**, 15674-15686.
12. A. K. Atmuri, G. A. Peklaris, S. Kishore and S. R. Bhatia, *Soft Matter*, 2012, **8**, 8965-8971.
13. A. S. Negi and C. O. Osuji, *Physical Review E*, 2010, **82**, 031404.
14. A. S. Negi and C. O. Osuji, *Phys. Rev. E*, 2009, **80**, 010404.
15. R. Bandyopadhyay, D. Liang, H. Yardimci, D. A. Sessoms, M. A. Borthwick, S. G. J. Mochrie, J. L. Harden and R. L. Leheny, *Phys. Rev. Lett.*, 2004, **93**.
16. H. Tanaka, S. Jabbari-Farouji, J. Meunier and D. Bonn, *Phys. Rev. E*, 2005, **71**, 021402.
17. S. Ali and R. Bandyopadhyay, *Langmuir*, 2013, **29**, 12663-12669.
18. W. Stumm, *Chemistry of the solid-liquid interface*, John Wiley & Sons, New York, 1992.
19. B. Ruzicka and E. Zaccarelli, *Soft Matter*, 2011, **7**, 1268-1286.
20. H. Z. Cummins, *J. Non-Cryst. Solids*, 2007, **353**, 3891-3905.
21. T. Nicolai and S. Cocard, *Langmuir*, 2000, **16**, 8189-8193.
22. A. Mourchid, E. Lecolier, H. Van Damme and P. Levitz, *Langmuir*, 1998, **14**, 4718-4723.
23. S. Jabbari-Farouji, H. Tanaka, G. H. Wegdam and D. Bonn, *Phys. Rev. E*, 2008, **78**, 061405-061410.
24. P. Mongondry, J. F. Tassin and T. Nicolai, *J.Colloid Interface Sci.*, 2005, **283**, 397-405.
25. B. Ruzicka, L. Zulian, R. Angelini, M. Sztucki, A. Moussaid and G. Ruocco, *Phys. Rev. E*, 2008, **77**, 020402-020404.
26. B. Ruzicka, L. Zulian, E. Zaccarelli, R. Angelini, M. Sztucki, A. Moussaïd and G. Ruocco, *Phys. Rev. Lett.*, 2010, **104**, 085701.
27. R. Angelini, E. Zaccarelli, F. A. de Melo Marques, M. Sztucki, A. Fluerasu, G. Ruocco and B. Ruzicka, *Nat Commun*, 2014, **5**, 4049.
28. B. Ruzicka, E. Zaccarelli, L. Zulian, R. Angelini, M. Sztucki, A. Moussaïd, T. Narayanan and F. Sciortino, *Nat Mater*, 2011, **10**, 56-60.
29. A. Shahin and Y. M. Joshi, *Langmuir*, 2010, **26**, 4219–4225.
30. D. Saha, R. Bandyopadhyay and Y. M. Joshi, *Langmuir*, 2015.
31. E. Paineau, I. Bihannic, C. Baravian, A. M. Philippe, P. Davidson, P. Levitz, S. S. Funari, C. Rochas and L. J. Michot, *Langmuir*, 2011, **27**, 5562-5573.

32. C. Abrahamsson, L. Nordstierna, J. Bergenholtz, A. Altskar and M. Nyden, *Soft Matter*, 2014, **10**, 4403-4412.
33. S. Letaief and E. Ruiz-Hitzky, *Chemical Communications*, 2003, 2996-2997.
34. H. J. M. Hanley, C. D. Muzny, D. L. Ho, C. J. Glinka and E. Manias, *International Journal of Thermophysics*, 2001, **22**, 1435-1448.
35. K. Sun, R. Kumar, D. E. Falvey and S. R. Raghavan, *J. Am. Chem. Soc.*, 2009, **131**, 7135-7141.
36. M. T. Shaw and W. J. MacKnight, *Introduction to Polymer Viscoelasticity*, Wiley, New York, 3 edition edn., 2005.
37. G. W. Becker, *Kolloid-Zeitschrift*, 1955, **140**, 1-32.
38. H. H. Winter and M. Mours, *Adv. Polym. Sci.*, 1997, **134**, 167.
39. H. H. Winter and F. Chambon, *Journal of Rheology*, 1986, **30**, 367-382.
40. S. Manley, B. Davidovitch, N. R. Davies, L. Cipelletti, A. E. Bailey, R. J. Christianson, U. Gasser, V. Prasad, P. N. Segre, M. P. Doherty, S. Sankaran, A. L. Jankovsky, B. Shiley, J. Bowen, J. Eggers, C. Kurta, T. Lorik and D. A. Weitz, *Physical Review Letters*, 2005, **95**, 048302.
41. H. Winter and M. Mours, *Advances in Polymer Science*, 1997, **134**, 165-234.
42. B. J. Adzima, H. A. Aguirre, C. J. Kloxin, T. F. Scott and C. N. Bowman, *Macromolecules*, 2008, **41**, 9112-9117.
43. M. Kaushal and Y. M. Joshi, *Macromolecules*, 2014, **47**, 8041-8047.
44. K. M. Schultz, A. D. Baldwin, K. L. Kiick and E. M. Furst, *Macromolecules*, 2009, **42**, 5310-5316.
45. S.-h. Hsu and A. M. Jamieson, *Polymer*, 1993, **34**, 2602-2608.
46. A. S. Negi, C. G. Redmon, S. Ramakrishnan and C. O. Osuji, *Journal of Rheology* 2014, **58**, 1557-1579.
47. A. Ponton, A. Bee, D. Talbot and R. Perzynski, *Journal of Physics Condensed Matter*, 2005, **17**, 821-836.
48. M. Muthukumar, *Macromolecules*, 1989, **22**, 4656-4658.
49. T. Matsumoto, M. Kawai and T. Masuda, *Macromolecules*, 1992, **25**, 5430-5433.
50. A. Ponton, S. Barboux-Doeuff and C. Sanchez, *Colloids and Surfaces A: Physicochemical and Engineering Aspects*, 2000, **162**, 177-192.
51. H. H. Winter, *Macromolecules*, 2013, **46**, 2425-2432.
52. S. Cocard, J. F. Tassin and T. Nicolai, *J. Rheol.*, 2000, **44**, 585-594.
53. S. Jatav and Y. M. Joshi, *Journal of Rheology*, 2014, **58**, 1535-1554.
54. F. Chambon and H. H. Winter, *Journal of Rheology*, 1987, **31**, 683-697.
55. S. Jatav and Y. M. Joshi, *Applied Clay Science*, 2014, **97–98**, 72-77.
56. W. Benenson, J. W. Harris, H. Stöcker and H. Lutz, *Handbook of Physics*, Springer-Verlag, New York, 2002.
57. P. B. Laxton and J. C. Berg, *Journal of Colloid and Interface Science*, 2006, **296**, 749-755.
58. F. Bergaya and G. Lagaly, eds., *Handbook of Clay Science*, Elsevier, Oxford, 2013.
59. J. C. Scanlan and H. H. Winter, *Makromolekulare Chemie. Macromolecular Symposia*, 1991, **45**, 11-21.
60. S. Mortimer, A. J. Ryan and J. L. Stanford, *Macromolecules*, 2001, **34**, 2973-2980.
61. J.-P. Eloundou, J.-F. Gerard, D. Harran and J. P. Pascault, *Macromolecules*, 1996, **29**, 6917-6927.
62. R. H. Colby, J. R. Gillmor and M. Rubinstein, *Physical Review E*, 1993, **48**, 3712-3716.

63. P. J. Lu and D. A. Weitz, *Annual Review of Condensed Matter Physics*, 2013, **4**, 217-233.